CIRCULATION DYNAMICS OF MEDITERRANEAN PRECIPITATION VARIABILITY 1948–98

A. DÜNKELOH and J. JACOBEIT*
Institute of Geography, University of Würzburg, Am Hubland, D-97074 Würzburg, Germany

ABSTRACT

Canonical correlation analysis is used to identify main coupled circulation–rainfall patterns and to relate recent variability and trends of Mediterranean precipitation to large-scale circulation dynamics. Analyses are based on geopotential heights (500 and 1000 hPa levels) for the North Atlantic–European area (National Centers for Environmental Prediction–National Center for Atmospheric Research reanalysis) and on highly resolved ($0.5^\circ \times 0.5^\circ$) monthly rainfall grids (Climatic Research Unit, Norwich) selected for the Mediterranean area during the 1948–98 period. Combining monthly analyses with similar characteristics to seasonal samples yields winter (October–March), spring (April–May) and summer (June–September) types of coupled variability; a particular autumn type for the whole Mediterranean does not occur on the monthly time scale. Coupled patterns specifically linked to one or two seasons include an east Atlantic jet (EA-Jet) related pattern for summer and a Mediterranean meridional circulation (MMC) pattern for winter and spring. The most important pattern recurring with dynamical adjustments throughout the whole year reflects the seasonal cycle of the Mediterranean oscillation (MO), which is linked (with seasonal dependence) to the Northern Hemisphere teleconnection modes of the Arctic oscillation (AO) and North Atlantic oscillation (NAO). Winter rainfall trends of the recent decades marked by widespread decreases in the Mediterranean area and by opposite conditions in the southeastern part are linked to particular changes over time in several of the associated circulation patterns. Thus, different regional rainfall changes are integrated into an overall interrelation between Mediterranean rainfall patterns and large-scale atmospheric circulation dynamics.

KEY WORDS: large-scale atmospheric circulation; Mediterranean precipitation; canonical correlation analysis (CCA); seasonal types of coupled variability

1. INTRODUCTION

The Mediterranean climate, extending in the transitional zone between the humid western and central European domain and the arid North African desert belt, is characterized by alternating circulation regimes linked to the dry and wet seasons throughout the year. Circulation dynamics include a high variability of precipitation on monthly, interannual and interdecadal time scales, strongly influencing regional water resources and water management. Therefore, a growing number of climate research studies published in the last few decades have focused on climate variability and change in the Mediterranean area.

Concerning rainfall variability, many recent studies have contributed results on a regional scale. Thus, for example, the Iberian Peninsula experienced a slightly dry period during the 1950s followed by a wetter period until the 1970s and a pronounced dry period since the 1980s (Esteban-Parra *et al*., 1998; González-Hidalgo *et al*., 2001; Goodess and Jones, 2002). Similar changes are known from the southwestern countries of Morocco and Algeria (Chbouki *et al*., 1995; Adjez, 2000). The central Mediterranean area, too, has experienced dry conditions during the last few decades. The decreasing rainfall trend in winter, however,

* Correspondence to: J. Jacobeit, Institute of Geography, University of Würzburg, Am Hubland, D-97074 Würzburg, Germany; e-mail: jucundus.jacobeit@mail.uni-wuerzburg.de

had started during the 1970s and was temporarily weakened by some wet years within the 1975–80 period (Conte *et al*., 1989; Buffoni *et al*., 1999; Brunetti *et al*., 2000).

Decreasing precipitation is also evident in large parts of the eastern Mediterranean area: time series from Greece, for example, show changes to drier conditions during the 1970s (further intensifying subsequently) after wetter conditions during the two decades before (Amanatidis *et al*., 1993; Kutiel *et al*., 1996a; Xoplaki *et al*., 2000). Similar developments are reported for the Mediterranean coast of Turkey (Türkes, 1996). In Cyprus, the period from the mid-1950s to the mid-1970s was at a low rainfall level compared with the first half of the 20th century (Kutiel *et al*., 1996a).

The opposite evolution is described for southern Israel (Ben-Gai *et al*., 1994, 1998; Steinberger and Gazit-Yaari, 1996), with a significant increase of precipitation during the last few decades, this being strongest at the beginning (October, November) and at the end (March) of the wet period. Further to the north this rainfall increase is no longer discernible, changing to rainfall decreases in northern Israel (Ben-Gai *et al*., 1994, 1998; Steinberger and Gazit-Yaari, 1996). The gridded rainfall data used in the present study reveal a slight increase of winter precipitation even in most areas along the south coast of the eastern Mediterranean between southern Israel and Libya. According to the European trend atlas based on station data (Schönwiese *et al*., 1994; Schönwiese and Rapp, 1997) and on trend analyses applied to gridded rainfall data (Jacobeit, 2000), the majority of the Mediterranean regions, however, have tended toward decreasing winter precipitation during the last few decades, mostly starting in the 1970s and proceeding to an accumulation of dry years in the 1980s and 1990s.

During spring, different recent rainfall trends are identified: increasing values in the northwestern region and in northern parts of the eastern Mediterranean (Schönwiese *et al*., 1994; Schönwiese and Rapp, 1997), and strongest decreases in the southwestern domain (Jacobeit, 2000). In early spring (March), strong negative rainfall trends are known from Iberia (Trigo and DaCamara, 2000) and strong positive trends from southern Israel (Ben-Gai *et al*., 1998). For autumn, too, non-uniform changes have recently been indicated: positive trends in western Iberia and on the south coast of Turkey (Jacobeit, 2000), and decreasing amounts in most areas of the western–central Mediterranean region (Schönwiese *et al*., 1994; Schönwiese and Rapp, 1997).

Looking at concomitant changes in the atmospheric circulation, a recent trend towards rising pressure, especially since the 1970s, is well documented for most of the Mediterranean area (e.g. Schönwiese *et al*., 1994; Reddaway and Bigg, 1996; Schönwiese and Rapp, 1997; Maheras *et al*., 2000; Brunetti *et al*., 2002). In particular, the strengthening during the winter months, both at the surface and at upper tropospheric levels, is highly significant, with the increase being most evident in the western to central Mediterranean area (Makrogiannis and Sashamanoglou, 1990; Schönwiese *et al*., 1994; Schönwiese and Rapp, 1997; Piervitali *et al*., 1997; Brunetti *et al*., 2002). This is related to the accumulation of positive modes of the North Atlantic oscillation (NAO) in winter during the last few decades (Hurrell and van Loon, 1997; Jacobeit *et al*., 2001). The changes in mean pressure fields are consistent with a weakening and a decreasing number of cyclones, as well as in an increasing number of anticyclones in the Mediterranean area during the rainy period (October–March) of the last few decades, being evident since the 1970s and strengthening during the 1980s and 1990s (Maheras *et al*., 2000, 2001; Trigo *et al*., 2000). This tendency is strongest in the western Mediterranean and weakens towards the central part, where the frequency of cyclones has not shown such a large decrease. The opposite development is reported for the Siberian anticylone, with its varying extension to eastern Europe (Sahsamanoglou *et al*., 1991): decades of a predominantly strong Siberian anticyclone from the 1950s to the 1970s are followed by a period since the 1980s with significantly weakened high pressure being related to a distinct temperature rise in this area. Schönwiese *et al*. (1994) and Schönwiese and Rapp (1997) show that decreasing pressure is a general feature during winter in the North Atlantic–European region north of 55 °N.

During spring, mostly insignificant pressure increases are identified in the Mediterranean area, with the greatest amounts in the southwestern and southeastern sector (Schönwiese *et al*., 1994; Schönwiese and Rapp, 1997; Brunetti *et al*., 2002). As an exception, early spring (March) shows significant pressure increases in the southwestern sector (e.g. Iberia) similar to the late winter months. For the summer season, increasing pressure across the western and central Mediterranean and decreasing pressure in upper tropospheric levels of the extreme eastern part have been identified (Meyrhöfer *et al*., 1996) embedded in the large-scale development

of decreasing pressure south of the Mediterranean and increasing pressure north of it (Kutiel and Kay, 1992). Autumn shows only a few significant pressure increases in the western–central domain (Schönwiese *et al*., 1994; Brunetti *et al*., 2002).

Finally, a further segment of investigations is focused directly on circulation–rainfall relationships. Earlier studies concerning rainfall variability (e.g. Meteorological Office, 1962; Reiter, 1975) were based on synoptic approaches for deriving particular circulation patterns. Since digital computer systems became generally available, nearly all empirical studies turned to statistical analyses of large datasets. Most of the studies, however, have a local or regional context, and only a few are related to the whole Mediterranean area. With respect to dynamic climatology, different objectives have been analysed: e.g. links between upper troughs and daily precipitation (Jacobeit, 1985, 1987) or the NAO influence on surface climate of the western and central Mediterranean (Lamb and Peppler, 1987; Zorita *et al*., 1992; Hurrell, 1995; Rodó *et al*., 1997; Esteban-Parra *et al*., 1998; Goodess and Jones, 2002). Thus, more frequent winter months with a positive NAO mode are strongly related to above-normal pressure and drier conditions in this region. Conte *et al*. (1989) first described the 'Mediterranean oscillation' (MO) as a teleconnection pattern with opposite pressure and rainfall anomalies between the western and eastern Mediterranean area, a pattern whose positive mode became stronger during the 1980s and 1990s. It was confirmed, even as the most important regional circulation–rainfall relationship, by studies based on a transect of stations throughout the Mediterranean basin (Kutiel *et al*., 1996b; Douguedroit, 1998; Maheras *et al*., 1999). Littmann (2000) developed an empirical weather classification for studying Mediterranean rainfall variability. Corte-Real *et al*. (1995) have already used canonical correlation analysis (CCA) for establishing coupled anomaly patterns between the large-scale circulation and Mediterranean precipitation. Their study, however, does not consider monthly or seasonal differences and disregards the patterns' time series. A similar analysis by Quadrelli *et al*. (2001) used gridded rainfall data but with a coarse spatial resolution ($2.5^\circ \times 2.5^\circ$); the link to hemispheric circulation data of three winter months (December–February) was established only for a short 16 year time period.

The present study is based on recently available gridded rainfall data (Section 2) appropriate for multidecadal analyses and for the detection of topographic influences on Mediterranean rainfall. It deals with coupled variations of circulation and precipitation and aims at attributing recent rainfall trends in different Mediterranean regions to the temporal evolution of particular large-scale circulation modes. In contrast to another simultaneously submitted paper based on station rainfall data, focusing on the winter season and including sea-surface temperatures and thickness grids of several tropospheric layers (see the similar study of Xoplaki *et al*. (2003) referring to summer temperatures), this study will be confined to the near-surface and an upper level of geopotential heights for representing the large-scale atmospheric circulation; but it extends the analyses to the whole seasonal cycle and arrives at the identification of seasonal circulation regimes, including seasonal types of coupled variability with Mediterranean precipitation. This follows former studies referring to separate monthly analyses (Dünkeloh and Jacobeit, 2001) and to the winter season in particular (Jacobeit and Dünkeloh, 2003). Thus, circulation–rainfall relationships will be presented for the whole Mediterranean area and for all seasonally different types of coupled variability.

2. DATA

Time series of geopotential height data are extracted from the National Centers for Environmental Prediction (NCEP)–National Center for Atmospheric Research (NCAR) reanalysis project (Kalnay *et al*., 1996; Kistler *et al*., 2001). These six-hourly data are available back to 1948 for several atmospheric levels on a $2.5^\circ \times 2.5^\circ$ grid. For the present study, monthly mean geopotential heights of the 1000 and 500 hPa levels were computed for the North Atlantic–European area 20–70 °N and 50 °W–40 °E, which includes 777 grid points.

Time series of highly resolved precipitation fields are provided by the Climatic Research Unit (CRU) in Norwich, UK. This monthly dataset is given on a $0.5^\circ \times 0.5^\circ$ grid for terrestrial areas and covers most of the 20th century (1901–98; New *et al*., 1999, 2000). It is based exclusively on station rainfall data but (in contrast to incomplete or inhomogeneous time series from individual stations) includes an optimized internal consistency. This is achieved by using anomalies with respect to a reference period (1961–90)

with a maximum number of stations and minimal cases of missing values. These anomalies, being highly representative on a regional scale, were submitted to thin-plate splines interpolation and to take into account the effects of topography (New *et al*., 2000). The resulting grid box values covering the Mediterranean area have proved to be of high quality due to the dense station network incorporated. For the present study, 1366 grid boxes have been selected as representing the main region of Mediterranean climate, including the Atlantic coastal areas to the west. Predominant rainfall during the winter half year at the northern margin and a rainfall minimum of 15 mm for most of the wet season months were used as criteria for the delimitation.

3. METHODS

CCA is applied to identify statistical relationships between the two sets of variables mentioned above. This method was originally developed from an interdependence model (Hotelling, 1936) and first applied in climatology during the 1980s (e.g. Barnett and Preisendorfer, 1987; Nicholls, 1987). A detailed description is given by von Storch and Zwiers (1999).

Pairs of spatial patterns (canonical loadings) are derived from two sets of variables in such a way that the correlation of their time coefficients (canonical scores) is maximized. Thus, each set of coupled patterns represents that part of the variance in both variable groups that is significantly correlated. The number of significant canonical correlations may be determined by Rao's F-test. Owing to the incorporation of two atmospheric levels (1000 and 500 hPa geopotential heights) within the group of circulation variables, each canonical correlation is spatially represented by a set of three coupled patterns (two for circulation and one for precipitation; see Xoplaki *et al*. (2003) for even more predictor variables). The associated time coefficients describe the temporal variation in polarity and strength of the corresponding spatial patterns.

Prior to the CCAs, the original fields of geopotential heights and Mediterranean precipitation were submitted to several kinds of pre-processing. First, each time series is transformed to absolute deviations from the long-term monthly mean (1948–98), respectively. Subsequently, principal component analysis (PCA) techniques (von Storch and Zwiers, 1999) were applied to reduce the dimensions of these transformed data and to obtain uncorrelated field variables. This kind of pre-processing removes noise from the original data and, at the same time, improves robustness and explained variances of the canonical patterns (being unoptimized by the CCA procedure itself). In the present study, unrotated PCAs (restraining the degree of pre-processing) were separately applied to the covariance matrices of geopotential heights and precipitation data, reducing each group to 11–12 principal components (PCs) with overall explained variances of 91–95% for geopotential heights and 67–71% for precipitation. These amounts correspond to orthogonally rotated PCA solutions with well-defined spatial centres of variation in each particular analysis (referring either to geopotential heights or to Mediterranean precipitation). But even retaining larger or smaller numbers of PCs would not essentially change the results of the subsequent CCAs for which the normalized PC scores are functioning as input variables.

Thus, to each final CCA, those numbers of PCs were put in which correspond to the above-mentioned decomposition into well-defined centres of variation. Furthermore, appropriate back-transformations allow patterns to be obtained in terms of anomalies according to the units of the original sets of variables (von Storch and Zwiers, 1999).

Initially, CCA patterns were calculated separately for each month. The main characteristics of these patterns, however, allow three major types to be distinguished throughout the whole year: a 'winter type', a 'spring type', and a 'summer type'. Despite some gradual transitions, most of the information from monthly analyses is retained by performing only three integrated analyses, with each month assigned to the seasonal type of primary importance. Thus, the analysis including all months from October to March (ONDJFM) reproduces the main winter-type characteristics; another one comprising all months from June to September (JJAS) reproduces the main summer-type characteristics. Finally, the residual months of April and May (AM) reflect a third common type associated with the spring season. The month of March might also be assigned to this spring type; differences between March and May, however, prove to be distinctly larger than those between March and the winter-type characteristics. A particular 'autumn type' for the whole Mediterranean area does not occur on the monthly scale, since September and October still reflect large parts of coupled variability

Table I. Number of extracted PCs and percentages of original variance (EV) accounted for by these PCs for geopotential heights (500 and 1000 hPa levels) and Mediterranean rainfall grids referring to winter (October to March), spring (April to May) and summer (June to September) analyses for the 1948–98 period

	PCs (EV)	
	Geopotential heights	Precipitation
Winter (ONDJFM)	12 (95.2%)	12 (71.1%)
Spring (AM)	12 (92.0%)	11 (70.9%)
Summer (JJAS)	11 (90.8%)	11 (66.8%)

constituting the summer and winter types, respectively. Table I summarizes numbers of input PCs together with overall explained variances for these three seasonal types of CCA.

4. RESULTS

4.1. Winter type of coupled variability

4.1.1. Canonical correlation patterns. For the months of the winter half year (October–March) eight highly significant (0.001 level) canonical correlation patterns (CCPs) could be extracted. Only five of them, however, prove to be robust in case of varying extensions of the study area or with changing numbers of input PCs. Furthermore, just these five patterns are typical for the winter season, insofar as they are largely reproduced by separate CCAs for the different months and for particular atmospheric levels. The remaining patterns six to eight (not shown) are neither robust nor typical in this sense and have only small canonical correlation coefficients ($r < 0.5$).

The first set of winter patterns W-CCP1 (Figure 1) with $r = 0.92$ includes by far the largest amounts of explained variance (EV; 30% for precipitation and 20% for geopotential heights). Both atmospheric levels are characterized by a pressure seesaw between the northerly subpolar zone and the region of southwestern Europe. Another centre of variation appears in the eastern Mediterranean at the 500 hPa level, which is reproduced even more distinctly when patterns are calculated in terms of correlation coefficients instead of real anomalies. The precipitation pattern shows opposite conditions between the whole western to central and the southeastern Mediterranean area.

The relationship between circulation and precipitation patterns is very reasonable from a synoptic and physical point of view: in the positive mode, high pressure over the southwestern region and an upper trough over the eastern Mediterranean lead to below-normal precipitation in most parts of the study area and to increased rainfall in some eastern parts, especially the coastal areas of Libya, Egypt, the Levant and the southern Aegean Sea exposed to the north or northwest, thus being affected by cool northerly winds passing over the eastern Mediterranean basin. In the negative mode, a trough around Great Britain–Iberia causes strong westerly airflow and advection of humid unstable air masses, especially affecting regions exposed to the west; east of the trough, dry North African air masses are directed towards the eastern Mediterranean, dominated by an anticyclonic ridge at the 500 hPa level.

W-CCP2 ($r = 0.89$) may be the most important one for many regions of the central to eastern Mediterranean area (Figure 1), explaining 20% and 8% of the total variances in precipitation and geopotential heights respectively. Owing to opposite centres of variation over the central Mediterranean and the eastern North Atlantic, predominantly meridional circulations will be established. The concomitant precipitation pattern shows a large anomaly field extending from Algeria through the whole central Mediterranean up to the south coast of Turkey; smaller domains with opposite anomalies exist at the Atlantic coast and towards the extreme southeastern part. This again implies a very reasonable relationship between circulation and precipitation

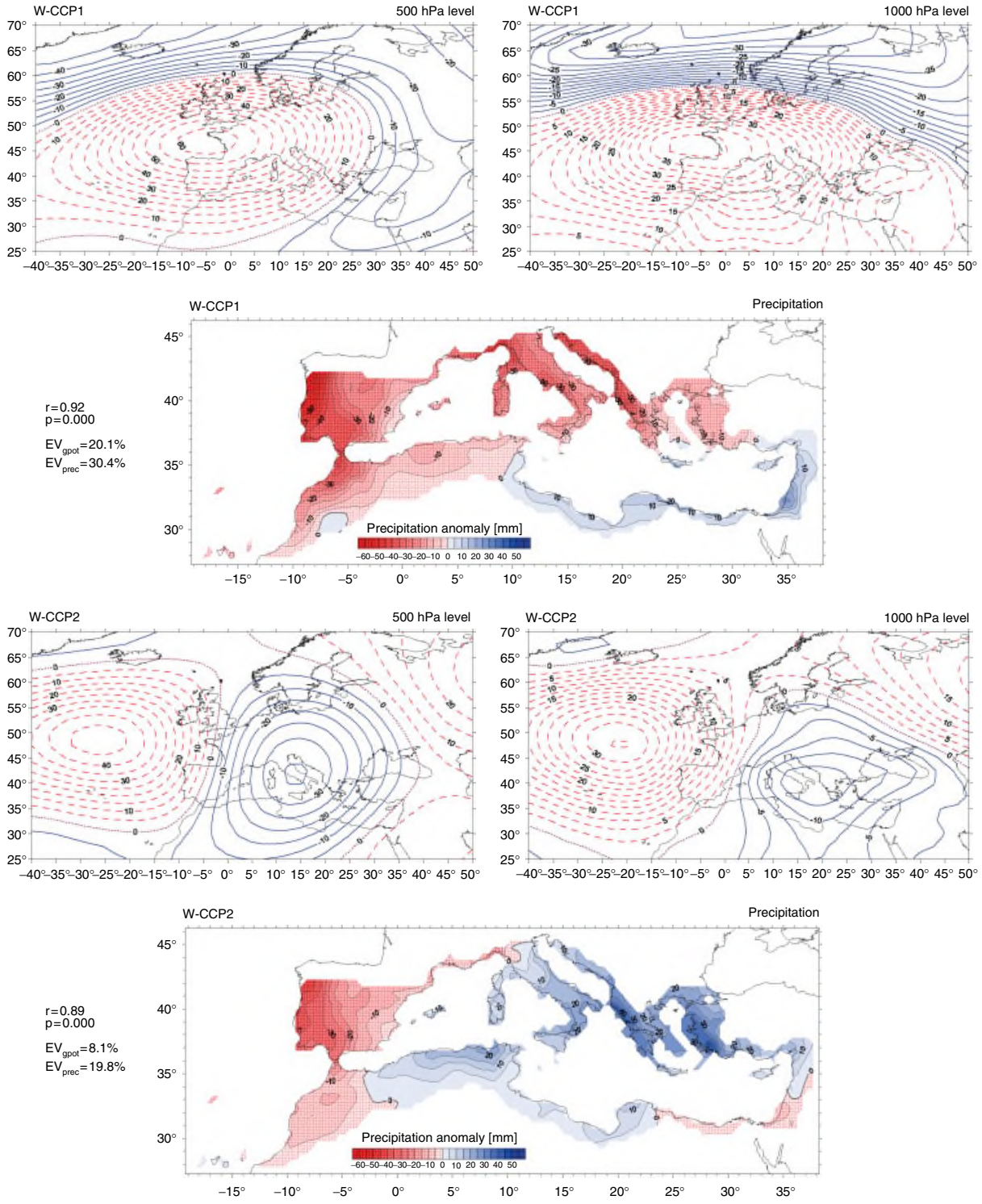

Figure 1. CCPs for winter (W-CCP) referring to geopotential heights at the 500 and 1000 hPa levels and to Mediterranean precipitation (October–March 1948–98). EV_{gpot}: explained variance, geopotential heights; EV_{prec}: explained variance, precipitation; r: canonical correlation coefficient; p: level of significance. This figure is available in colour online at http://www.interscience.wiley.com/ijoc/

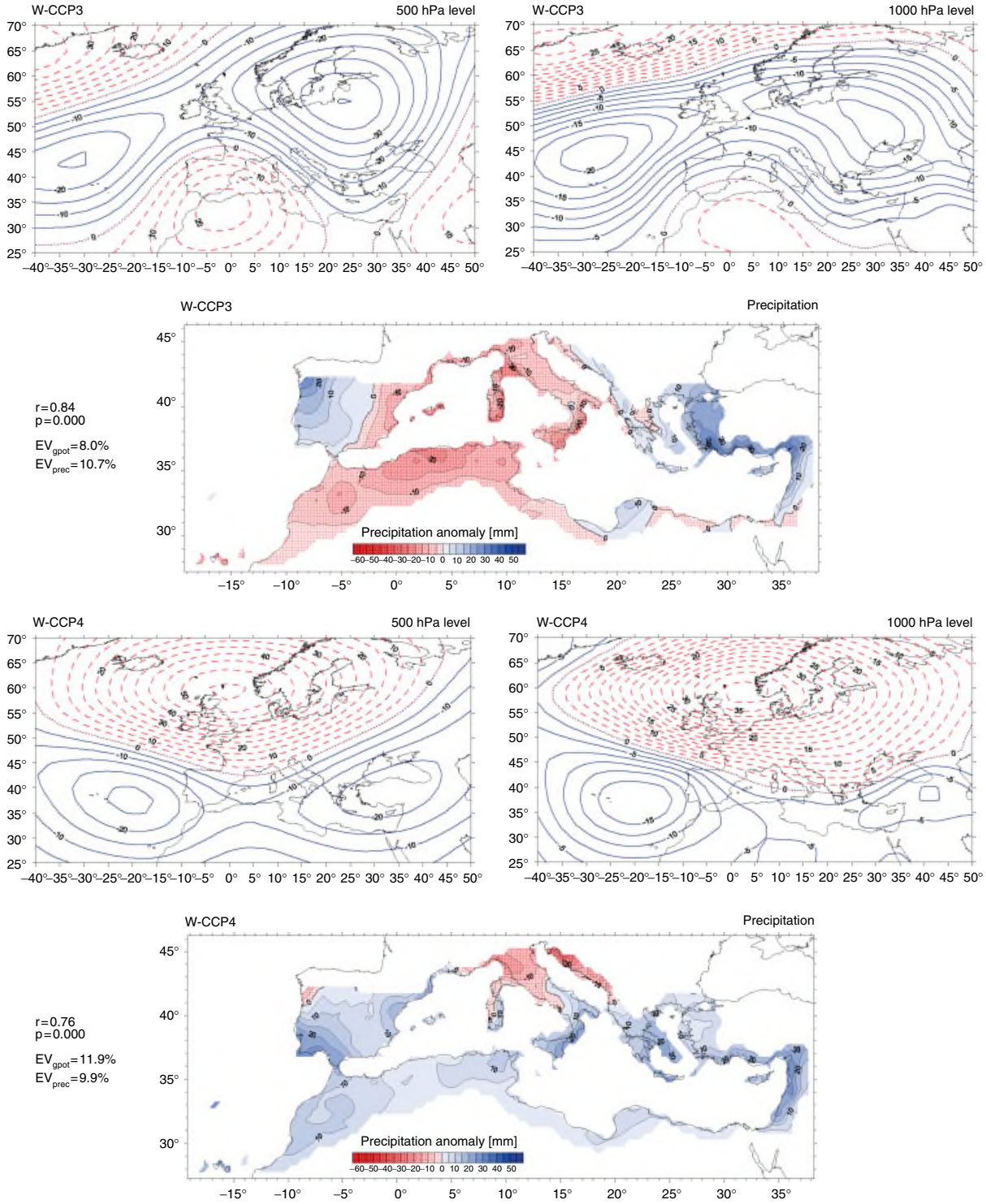

Figure 1. (*Continued*)

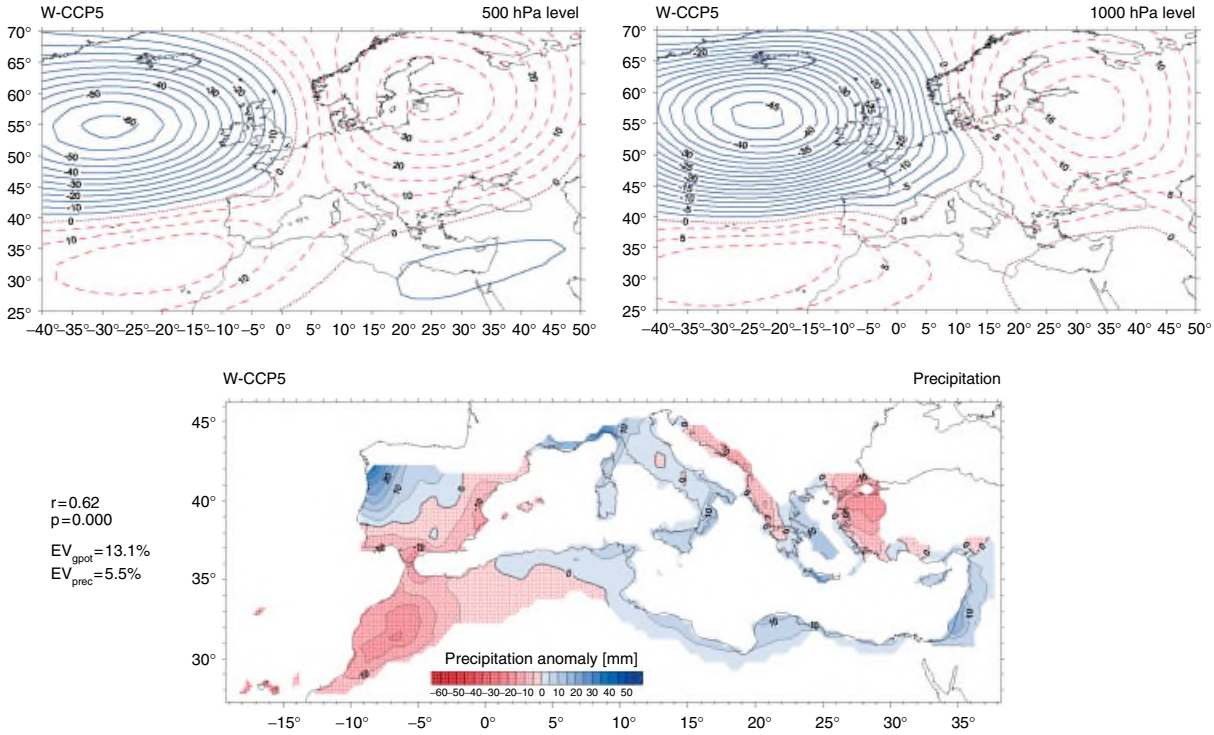

Figure 1. (*Continued*)

anomalies: in the positive mode, a meridional trough extending from central Europe to North Africa includes advection of subpolar air masses by northerly flow and Mediterranean cyclogenesis; precipitation increases, especially on coasts exposed to the north/northwest within the northerly airflow (Algeria, Tunisia) and to the west/southwest within the frontal airflow downstream (western Greece and Turkey). At the same time, the Atlantic margin experiences anticyclonic conditions and below-normal precipitation. In the negative mode, however, it is affected by cyclonic westerlies related to an eastern North Atlantic trough, whereas most of the Mediterranean region receives below-normal rainfall due to anticyclonic conditions.

W-CCP3 ($r = 0.84$) explains 10% and 8% of the total variances of precipitation and geopotential heights, respectively. Its circulation (Figure 1) is dominated by a large-scale anomaly extending from the eastern North Atlantic to a distinct centre in eastern Europe, which also marginally affects the eastern Mediterranean. Opposite anomalies, especially at the 500 hPa level, exist near Greenland, above north-west Africa and the Near East. The precipitation pattern reveals an extensive anomaly zone over the western and central Mediterranean, in contrast to smaller areas with opposite sign at the northern border of the eastern Mediterranean and the extreme northwestern part of Iberia. In the positive mode, the cyclonic westerlies are kept away from the western Mediterranean by an anticyclonic wave around these longitudes; above-normal precipitation only occurs to the northwest of Iberia. The downstream trough over eastern Europe does affect the Mediterranean precipitation pattern, with the region of above-normal rainfall shifted somewhat to the east compared with the second pattern discussed earlier. In the negative mode, however, a high pressure influence dominates this region, with blocking effects leading to positive rainfall anomalies around the western Mediterranean basin.

W-CCP4 ($r = 0.76$), explaining 12% and 10% of the total variances respectively, represents a typical seesaw between the northern and the southern latitudes, with centres of variation over the North Sea and around the western and eastern domains of the subtropical belt (Figure 1). The corresponding precipitation pattern is dominated by a widespread anomaly covering nearly the whole Mediterranean area except for a small northern section in the central part. The positive mode is characterized by a strong blocking action in higher latitudes

linked with cyclonic conditions to the south, reaching maxima with above-normal rainfall at the Atlantic margin and around the eastern Mediterranean favoured by cold air advection from northeasterly regions. The negative mode, in contrast, implies Mediterranean anticyclonicity with below-average precipitation; at the same time, central Europe is dominated by cyclonic westerly flow, which also affects the most northern parts of the central Mediterranean region, in particular those exposed to the west.

W-CCP5 ($r = 0.62$) explains the largest amount (apart from the first mode) of geopotential height variance (13%), but only a small part of the Mediterranean rainfall variance (5.5%). Four centres of variation constitute the circulation patterns: two opposite centres over the northern and southern latitudes, including an inverse polarity within both the western and eastern longitudinal sections. The southern centres would appear distinctly stronger within patterns calculated in terms of correlation coefficients instead of real anomalies.

4.1.2. Temporal variability. The normalized time coefficients of the CCPs describe their month-to-month variations with respect to polarity and strength. Owing to their high canonical correlation ($r = 0.92$), circulation and precipitation patterns of W-CCP1 show a nearly simultaneous variability in time (Figure 2). A significant upward trend according to the Mann–Kendall test (Table II) is superimposed on these variations, not due to a continuous increase, however, but to distinct periods of opposite conditions: dominating negative modes in the early decades (especially during the 1960s) in contrast to frequently positive modes in the 1980s and 1990s. Figure 2 indicates the mean values for these subperiods differing significantly (0.1% level) according to the Mann–Whitney test. The 1970s may be seen as a transitional period.

The temporal evolution of W-CCP2 is only affected by one major change around 1988, starting a period with predominantly negative modes; this is reflected by significantly different mean values before and after this time (Figure 2) and by a significantly negative trend in the second half of the time series (Table II). W-CCP3 does not show any distinct anomalies or abrupt changes during the study period. Completely different conditions are indicated for W-CCP4: despite a lower correspondence in details ($r = 0.76$), both patterns distinctly reflect a remarkable change during the 1970s from preferred positive to negative values with significantly different mean values during these subperiods (Figure 2) and the most significant trend for the whole study period (Table II). Time coefficients of W-CCP5 show a preference for positive anomalies from the 1970s to the mid-1980s and negative ones after this time (Figure 2) without, however, producing any significant trend (Table II).

4.2. Spring type of coupled variability

4.2.1. Canonical correlation patterns. The spring (SP) analysis for the April–May period yields five significant CCPs; only three of them, however, proved to be robust and will be considered further. In contrast to the other seasons, there are two leading patterns, each accounting for roughly the same percentages (nearly 20%) of the rainfall variance in spring. This season contributes much less than winter to the annual rainfall of large-scale regions, but its circulation regime has to be considered as a particular one between winter and summer.

SP-CCP1 ($r = 0.88$; $EV_{prec} = 19.3\%$; $EV_{gpot} = 12.2\%$) is the most intrinsic spring pattern characterized by a northwest–southeast sequence of variation centres extended along southwest–northeast axes (especially at the upper level; see Figure 3). According to the major centres, this spring-type configuration might be a seasonal modification of W-CCP2. The central Mediterranean centre is directly linked with rainfall variability in large areas of the Mediterranean region; only the western part of the Iberian Peninsula reflects the opposite pressure variation above the North Atlantic Ocean. Another change in sign is indicated for the Levant region according to the second opposite centre aloft. In the positive mode, the Atlantic domain is governed by a blocking high with a strong cyclonic regime centred above the Mediterranean. In the negative mode, a central Mediterranean anticyclone prevents Atlantic low-pressure systems from penetrating to these interior parts.

SP-CCP2 ($r = 0.85$; $EV_{prec} = 19.8\%$; $EV_{gpot} = 10.5\%$) represents opposite conditions between western and eastern regions linked with a zonally symmetric pressure seesaw (Figure 3), thus resembling W-CCP1 to a large extent. In contrast to that one, however, the western centre in spring is shifted towards the Bay of Biscay, influencing rainfall variability from the Atlantic margin up to the Adriatic Sea; most parts of the

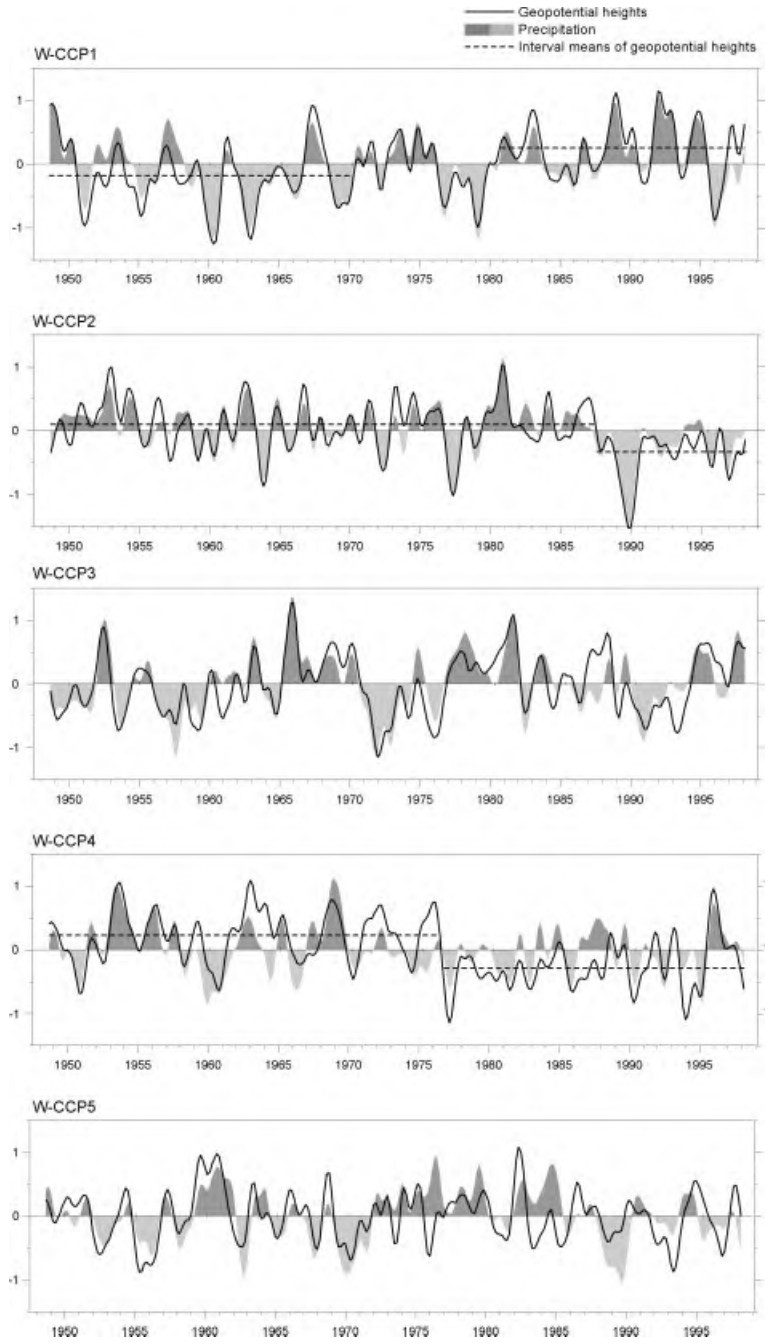

Figure 2. Smoothed series (Gaussian low-pass filter period 10 years) of time coefficients referring to the winter CCPs (W-CCP) of Figure 1. Dashed lines indicate mean values for particular intervals differing significantly at the 0.1% level (Mann–Whitney test)

African domain and the eastern Mediterranean area are affected by the weaker pressure centre (upper level) in the eastern section. The positive mode represents a zonal circulation pattern with a cyclonic wave further downstream; the negative mode implies reversals with cyclonic activity located in the southwestern region.

SP-CCP3 ($r = 0.79$; $EV_{prec} = 15.9\%$; $EV_{gpot} = 7.0\%$) includes a large anomaly zone from the Atlantic Ocean to eastern Europe still affecting rainfall variability in the northern part of the central Mediterranean

Table II. Linear trends of the time coefficients of seasonal CCPs with respect to the whole period 1948–98 and to particular subperiods with significant trends. W: winter; SP: spring; S: summer

Pattern	Period	Linear trend	Mann–Kendall test value
W-CCP1	1948–98	0.49	2.31*
W-CCP2	1948–98	−0.38	−1.79
	1973–98	−0.61	−1.98*
W-CCP3	1948–98	0.29	1.60
W-CCP4	1948–98	−0.65	−3.47**
W-CCP5	1948–98	−0.08	−0.48
SP-CCP1	1948–98	0.02	−0.15
SP-CCP2	1948–98	−0.39	−0.91
SP-CCP3	1948–98	0.46	1.32
S-CCP1	1948–98	−0.05	−0.54
	1948–78	1.06	3.89**
	1968–98	−0.80	−3.09**
S-CCP2	1948–98	−0.25	−0.86
S-CCP3	1948–98	−0.02	0.13

* Significant at the 5% level;
** Significant at the 1% level.

area; further to the south, opposite deviations prevail, with two centres southwest of Spain and in the Near East (Figure 3). The positive mode represents widespread anticyclonic conditions in the Mediterranean area (except for the northern central part); the negative mode implies some instability with a preference to the southwest.

4.2.2. Temporal variability. Generally, the spring time series (Figure 4) do not include significant trends (Table II), but they do exhibit some particular anomaly periods. Thus, SP-CCP1 preferred negative modes during the 1960s and 1980s, whereas strong opposite anomalies occurred during the 1970s and at the beginning of the 1990s. SP-CCP2 showed some preference for positive modes during the earlier decades and for negative modes during the 1980s. Finally, SP-CCP3 reveals a change around 1977 from negative modes preferred one decade earlier to positive modes in the following period. Longer term trends, however, are not established by these decadal-scale variations.

4.3. Summer type of coupled variability

4.3.1. Canonical correlation patterns. Most areas around the eastern Mediterranean basin do not experience substantial summer precipitation, and thus are excluded from further analysis (i.e. the summer rainfall patterns are only based on 851 (instead of 1366) grid boxes for the Mediterranean region). The summer (S) analysis for the months of June to September yields three sets of significant and robust CCPs.

S-CCP1 ($r = 0.75$; $EV_{prec} = 29.6\%$; $EV_{gpot} = 16.7\%$) includes by far the biggest circulation influence on summer rainfall for most of the Mediterranean regions and represents the most characteristic summer-type patterns of coupled variability. Pressure deviations are zonally organized, with a southern axis from Iberia towards the Black Sea and a northern axis from the Atlantic Ocean towards the Baltic Sea (Figure 5). The corresponding rainfall pattern has strongest deviations in those (northern Mediterranean) regions where the highest mean rainfall is recorded during summertime. The positive mode includes high pressure in mid to northern latitudes and unstable conditions to the south, with anomalous rainfall in the northern part of the central to northeastern Mediterranean region. The negative mode implies distinctly dry Mediterranean conditions, whereas low pressure prevails in northern Europe.

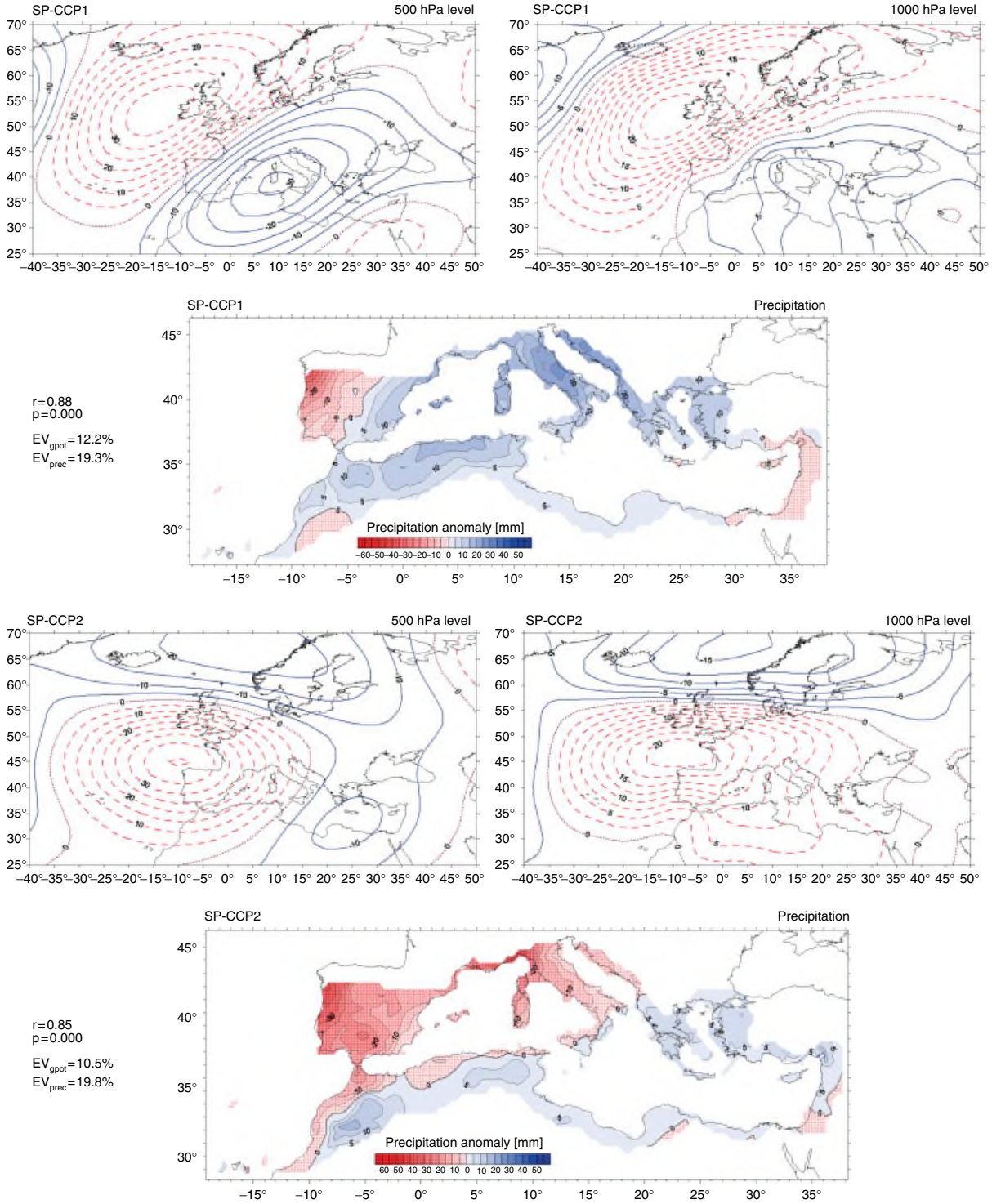

Figure 3. CCPs for spring (SP-CCP) referring to geopotential heights at the 500 and 1000 hPa levels and to Mediterranean precipitation (April–May 1948–98). EV$_{gpot}$: explained variance, geopotential heights; EV$_{prec}$: explained variance, precipitation; r: canonical correlation coefficient; p: level of significance. This figure is available in colour online at http://www.interscience.wiley.com/ijoc/

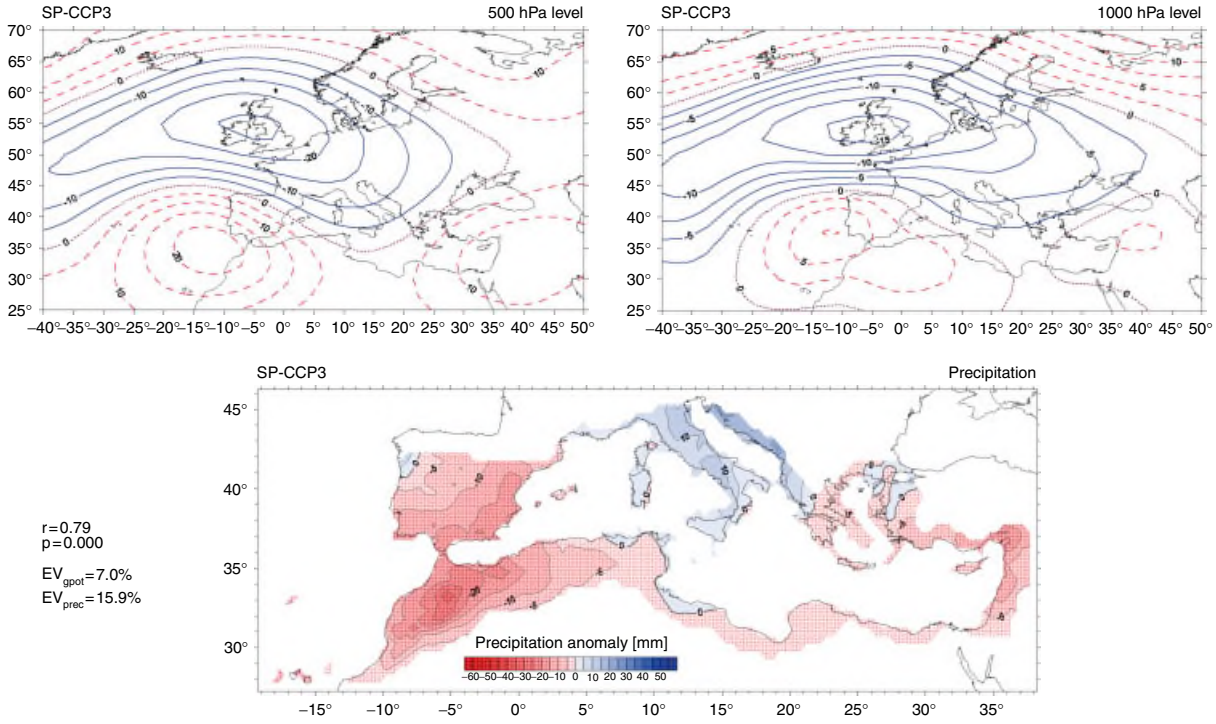

Figure 3. (*Continued*)

S-CCP2 ($r = 0.67$; $EV_{prec} = 10.1\%$; $EV_{gpot} = 12.2\%$) has some resemblance to SP-CCP2, but with the western centre of variation shifted from the Bay of Biscay towards the British Isles (Figure 5). At the upper level the opposite centre is still indicated, now displaced to the southern-central Mediterranean region. A direct influence of the western centre on the corresponding rainfall pattern is confined to the western margin of the Iberian Peninsula and to small areas at the northern border of the central Mediterranean region.

S-CCP3 ($r = 0.57$; $EV_{prec} = 14.3\%$; $EV_{gpot} = 6.3\%$) appears as a modulation of SP-CCP3 with weakened and slightly displaced centres of variation (located further north or northeast respectively). The corresponding rainfall pattern still indicates opposite conditions between the Iberian Peninsula and the Adriatic domain (Figure 5), but due to very low precipitation amounts there are no longer further centres around northwestern Africa and the eastern Mediterranean area.

4.3.2. Temporal variability. The summer time series (Figure 6) do not show any significant trend for the whole period since the mid-20th century (Table II). Most conspicuous are some different anomaly periods in S-CCP1: generally higher values during the 1960s and 1970s than previously and recurring negative values between 1980 and 1994, with corresponding mean values differing significantly at the 0.1% level between these successive intervals (Figure 6). When calculating linear trends for the first and the second half of the time series, these differences even lead to significant trends with opposite sign during these intervals (Table II). However, another change to preferred positive S-CCP1 modes is recently indicated for the mid-1990s.

5. DISCUSSION

5.1. Winter type

The first set of canonical correlation patterns for winter (W-CCP1) accounting for the largest part of Mediterranean rainfall variance represents an oscillating system with prevailingly opposite pressure (especially

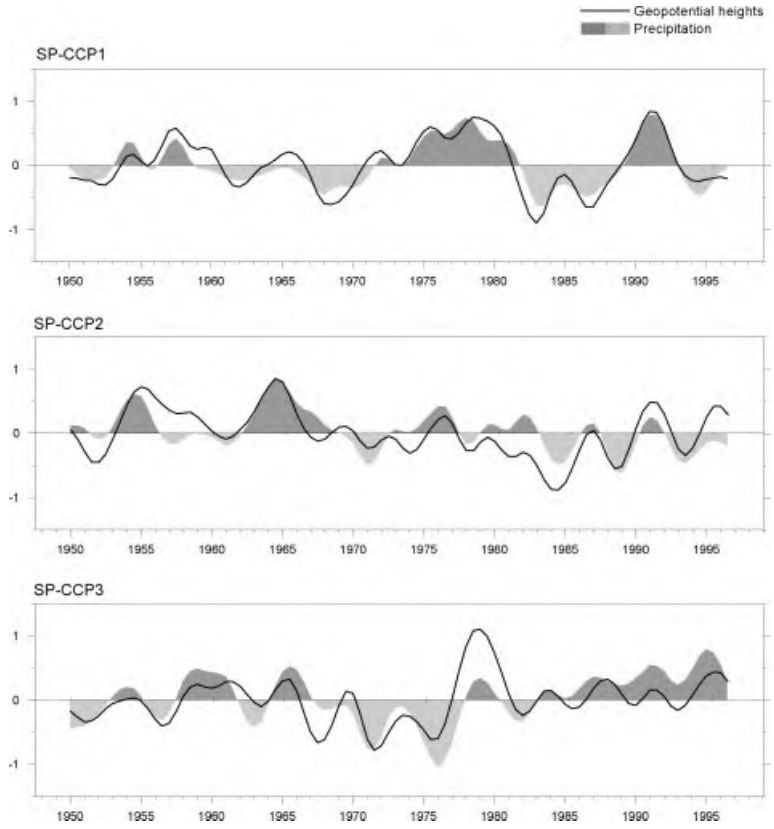

Figure 4. Smoothed series (Gaussian low-pass filter period 10 years) of time coefficients referring to the spring CCPs (SP-CCP) of Figure 3

at upper levels) and surface climate conditions between the western to central and the eastern Mediterranean basin. The existence of such a regional dynamic system and its impact on surface climate variability have already been described in several earlier studies (e.g. Conte *et al*., 1989; Corte-Real *et al*., 1995; Palutikof *et al*., 1996; Piervitali *et al*., 1997; Douguedroit, 1998; Kutiel and Paz, 1998; Maheras *et al*., 1999; Brunetti *et al*., 2002; Palutikof, 2003; Xoplaki *et al*., 2003) and referred to as the MO.

Looking at the correlations between Northern Hemisphere teleconnection indices and the seasonal CCP time series (Table III) reveals that W-CCP1 is significantly correlated with various indices of the Arctic oscillation (AO; Thompson and Wallace, 2000) and of the NAO, both from station time series (Hurrell, 1995; Jones *et al*., 1997) and from empirical orthogonal function (EOF)/PC analyses by the National Oceanic and Atmospheric Administration Climate Prediction Center (NOAA–CPC, 2003). Thus, the MO turns out to be a regional pattern with strong dependence on AO/NAO, confirming their large influence on Mediterranean winter rainfall variability. The importance of NAO-related patterns for surface climate variability in the western Mediterranean area is well known from many regional dynamic studies, e.g. for Iberia (von Storch *et al*., 1993; Goodess and Jones, 2002), Portugal (Corte-Real *et al*., 1998; Trigo and DaCamara, 2000), Spain (Zorita *et al*., 1992; Rodó *et al*., 1997; Esteban-Parra *et al*., 1998) and Morocco (Lamb and Peppler, 1987; Chbouki *et al*., 1995). In particular, the first canonical pair of winter (December–February) mean sea-level pressure (SLP) in the North Atlantic and of observed Iberian winter rainfall (Zorita *et al*., 1992; von Storch *et al*., 1993) represents the typical influence of an NAO-related pattern on westernmost Mediterranean precipitation variability. The fact that circulation patterns of W-CCP1 do not coincide completely with ordinary NAO patterns is due to the inherent coupling with rainfall variability throughout the whole Mediterranean area, i.e. W-CCP1 represents those parts of the AO/NAO constituting the regionally scaled MO.

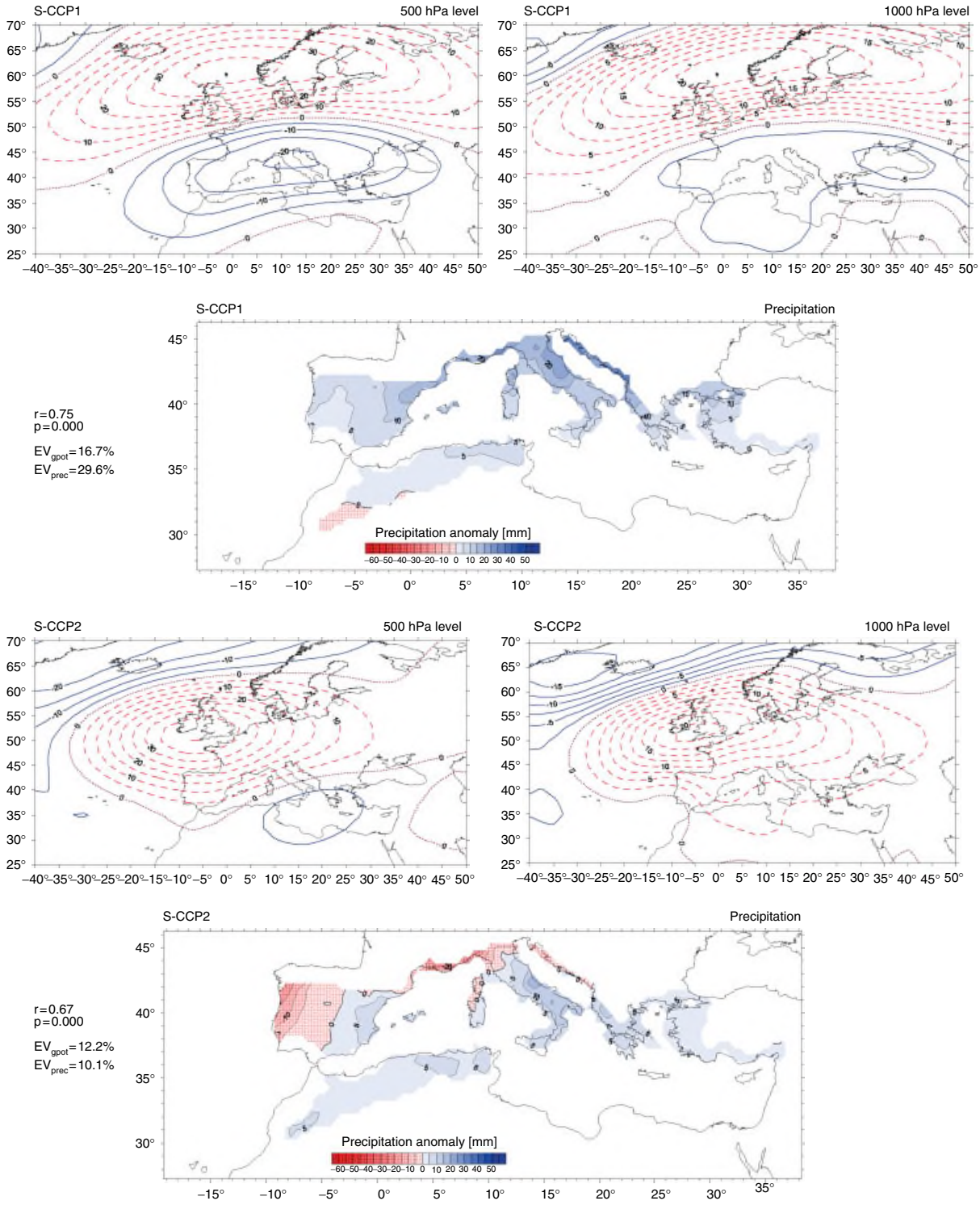

Figure 5. CCPs for summer (S-CCP) referring to geopotential heights at the 500 and 1000 hPa levels and to Mediterranean precipitation (June–September 1948–98). EV_{gpot}: explained variance, geopotential heights; EV_{prec}: explained variance, precipitation; r: canonical correlation coefficient; p: level of significance. This figure is available in colour online at http://www.interscience.wiley.com/ijoc/

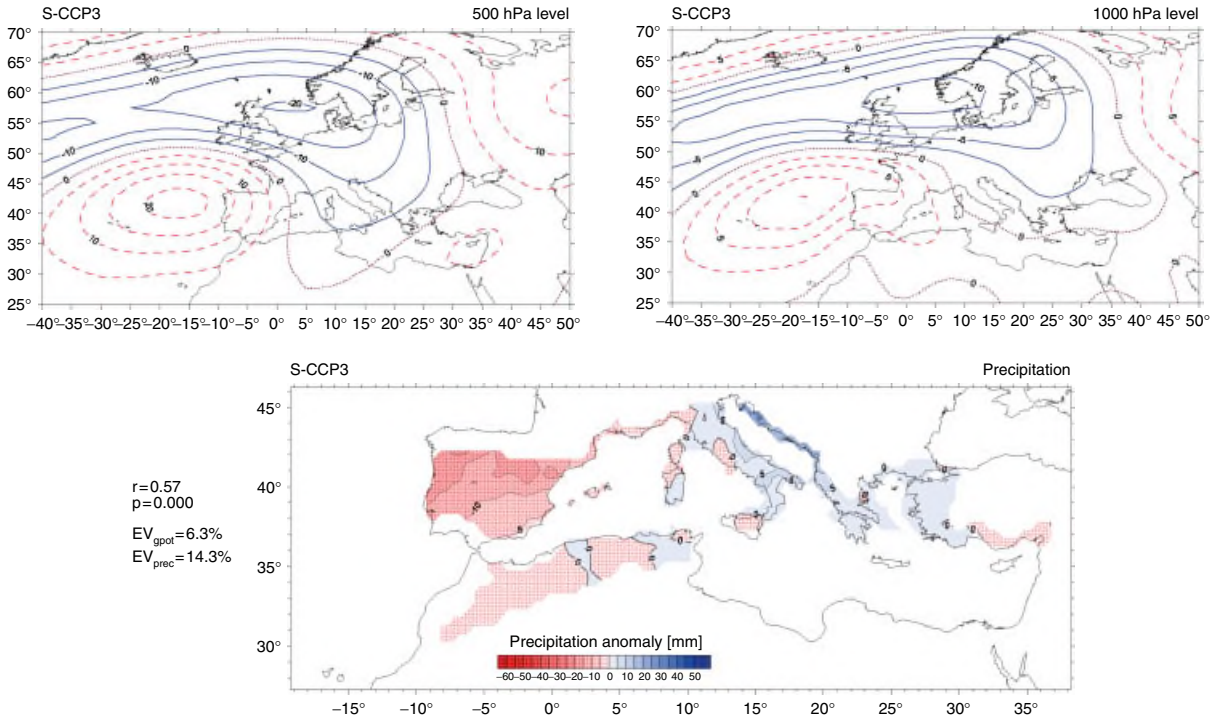

Figure 5. (*Continued*)

Similar to the NAO, various indices based on station pressure time series were proposed to describe the MO (Table IV). W-CCP1 is highly correlated to these indices, especially at the 500 hPa level. Spatially fixed station indices, however, are not able to consider movements of the centres of variation according to the seasonal cycle. Therefore, time coefficients from analyses of large-scale circulation patterns are often preferred. Concerning regional phenomena (like the MO) being linked to hemispheric modes, CCA is an appropriate method owing to its focus on the most important modes of coupled variability. Thus, W-CCP1 typically depicts the MO as being the most important coupled mode for winter, and a similar result is achieved even for the case of a whole-year analysis (Corte-Real *et al*., 1995). Concerning SLP–precipitation relationships for the whole of Europe, a slightly modified CCA pattern was derived by Qian *et al*. (2000) in the second mode, implying that the corresponding pattern only dominates in a Mediterranean climate context.

Further regional results are consistent with flow characteristics of W-CCP1: e.g. the close connection of northerly to westerly flow with Israeli precipitation described by Kutiel *et al*. (1996a,b), Kutiel and Paz (1998) and Krichak *et al*. (2000) is an integral part of the positive MO mode with its upper trough in the eastern Mediterranean region. In the negative MO mode, hot and dry air masses enter this eastern domain (Kutiel and Paz, 1998; Krichak *et al*., 2000) whereas unstable conditions under westerly airflow prevail further to the west.

The temporal evolution of the MO pattern (W-CCP1 in Figure 2) contributes to an increase of high pressure circulation types in the southwestern sector and decreasing winter precipitation in large parts of the western and central Mediterranean area. The southeastern sector, however, is favoured by increasing northerly winds with positive rainfall deviations.

Regional cyclogenesis and cyclone tracks have an important influence on Mediterranean rainfall conditions (Alpert *et al*., 1990; Flocas and Giles, 1991; Trigo *et al*., 1999; Maheras *et al*., 2001) and are strongly related to the prevailing circulation regime. W-CCP2, accounting for the largest part of winter rainfall variance in major areas of the northeastern and southern-central Mediterranean domain, is favourable (in its positive mode) to regional cyclogenesis and to depressions moving on typical tracks from the western

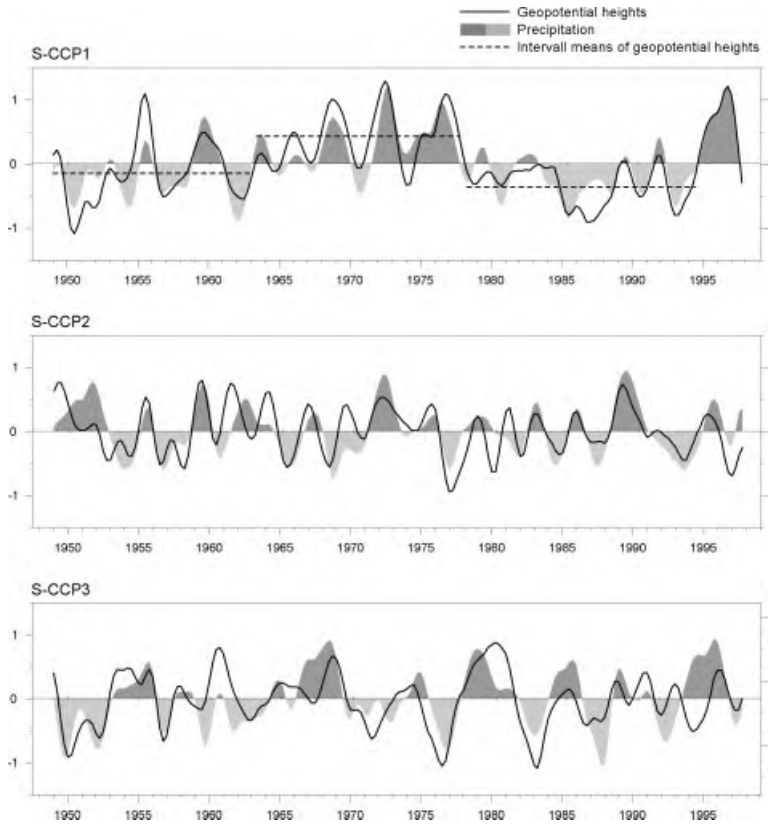

Figure 6. Smoothed series (Gaussian low-pass filter period 10 years) of time coefficients referring to the summer CCPs (S-CCP) of Figure 5. Dashed lines indicate mean values for particular intervals differing significantly at the 0.1% level (Mann–Whitney test)

Mediterranean basin towards the Aegean Sea. This is linked with a meridional trough pattern at upper levels. The connection of high precipitation in the Aegean Sea with southern meridional flow and a trough extending to the central Mediterranean has also been revealed within several studies on a regional scale (e.g. Kutiel *et al*., 1996a,b; Xoplaki *et al*., 2000). Being a dominant pattern (beyond the MO) coupled with Mediterranean climate variability, W-CCP2 is suggested for the acronym 'Mediterranean meridional circulation' (MMC) pattern referring to the prevailing meridional flows in the area of regional cyclogenesis. The MMC pattern is defined by two opposite pressure centres of variation: one core is west of Great Britain, near 45–50 °N and 20–25 °W; the other core is in the central Mediterranean, near the Italian peninsula (often more distinct in upper tropospheric levels; see Figure 1). The MMC pattern shows some correlation with the east Atlantic (EA) teleconnection pattern (Table III), probably due to the centre of variation in the northern Atlantic. Its prominent importance for Mediterranean climate variability is confirmed by its recurrence within further CCA studies, e.g. as second mode of the whole-year analysis by Corte-Real *et al*. (1995) or as first mode of the Greek winter rainfall analysis by Xoplaki *et al*. (2000).

The accumulation of strong negative anomalies in the time series of the MMC pattern since 1988 (Figure 2) implies a weakening of the trough extending into the central Mediterranean and a corresponding weakening of regional cyclogenesis linked with the positive mode of this circulation pattern. This is consistent with Maheras *et al*. (2000) pointing out that the general decrease of cyclone frequency since the 1970s became evident in the central Mediterranean not before the late 1980s. This might be due to prevailingly positive modes of the MMC pattern before 1988 supporting cyclonic activity in the central and northeastern Mediterranean area. Subsequently, some very dry years, such as 1989 (Türkes, 1996), were experienced in the central regions and northern parts of the eastern Mediterranean, possibly linked to a high influence of negative MMC modes.

Table III. Correlation coefficients r between Northern Hemisphere teleconnection indices and the time coefficients of seasonal CCPs for the period 1948–98 (1950–98 for the NOAA–CPC indices). W: winter; SP: spring; S: summer; figures in bold: $r \geq 0.4$

	W-CCP1	W-CCP2	W-CCP3	W-CCP4	W-CCP5	SP-CCP1	SP-CCP2	SP-CCP3	S-CCP1	S-CCP2	S-CCP3
NAO (Jones, 2003)	**0.72****	0.10	−0.14*	−0.23**	0.39**	−0.10	**0.55****	0.19*	−0.32**	**0.45****	0.24**
NAO (Hurrell, 2003)	**0.49****	0.23**	**−0.41****	−0.27**	0.31**	0.25**	0.30**	−0.04	−0.05	0.27**	0.25**
NAO (NOAA–CPC, 2003)	**0.45****	0.24**	−0.35**	−0.07	0.15*	0.31**	0.18	−0.14	0.27**	**0.52****	−0.27**
AO (Thompson and Wallace, 2003)	**0.60****	−0.07	−0.39**	0.02	0.15*	0.13	0.31**	−0.31**	−0.06	**0.45****	−0.10
EA (NOAA–CPC, 2003) pattern	0.13*	−0.38**	0.17**	−0.33**	**0.43****	–	–	–	–	–	–
EA-Jet (NOAA–CPC, 2003)	–	–	–	–	–	−0.21*	0.29**	**0.44****	**−0.66**[a]	0.10[a]	0.31**[a]

* Significant at the 5% level; (t-test; some few deviations from normal distribution and some significant autocorrelations have been considered by Fisher's transformation and by reductions in the number of degrees of freedom respectively).
** Significant at the 1% level.
[a] For June–August.

Table IV. Correlation coefficients r between regional Mediterranean teleconnection indices and the time coefficients of seasonal CCPs for the 1948–98 period. W: winter; SP: spring; S: summer; MOI: Mediterranean oscillation index; MPI: Mediterranean pressure index; MCI: Mediterranean circulation index figures in bold: $r \geq 0.4$. The Mediterranean indices (originally defined with station pressure time series) have been recalculated with NCEP–NCAR reanalysis data (500 and 1000 hPa levels)

	W-CCP1	W-CCP2	W-CCP3	W-CCP4	W-CCP5	SP-CCP1	SP-CCP2	SP-CCP3	S-CCP1	S-CCP2	S-CCP3
MOI[a]	**0.76****	−0.35**	0.24**	0.19**	0.22**	**−0.65****	**0.49****	−0.23*	**−0.47****	0.10	−0.26**
500/1000 hPa level	**0.52****	0.32**	0.20**	0.19**	0.14*	0.07	**0.56****	0.13	**−0.43****	0.29**	0.21**
MPI[b]	**0.81****	−0.16**	0.26**	0.15*	0.32**	**−0.45****	**0.61****	−0.05	**−0.44****	0.16	0.00
500/1000 hPa level	**0.50****	0.38**	0.26**	0.02	0.26**	−0.03	0.38**	0.26**	−0.33**	0.04	0.10
MCI[c]	**0.81****	−0.34**	−0.01	0.34**	0.19**	**−0.46****	**0.49****	**−0.49****	**−0.40****	0.35**	−0.33**
500/1000 hPa level	**0.60****	0.17**	0.11	**0.42****	0.05	−0.08	**0.58****	−0.31**	**−0.41****	**0.43****	0.05

* Significant at the 5% level; (t-test; same as in Table III).
** Significant at the 1% level.
[a] Difference of normalized geopotential height anomalies at Algiers and Cairo (Conte *et al*., 1989).
[b] Difference of normalized pressure anomalies at Gibraltar and Lod/Israel (Palutikof, 2003).
[c] Difference of normalized pressure anomalies at Marseille and Jerusalem (Brunetti *et al*., 2002).

At the same time, the eastern North Atlantic trough directing maritime air masses to the western and central parts of the Iberian peninsula, compensates for some of their latest rainfall losses due to W-CCP1.

W-CCP3 and W-CCP4 account for smaller parts of rainfall variance, but are still important for some areas of the southern-central Mediterranean (Tunisia, Malta, southeastern coasts of Italy), where the first two winter patterns do not correspond well to a reasonable circulation–rainfall relationship. Kutiel *et al*. (1996b), for example, revealed that the wettest conditions in Luqa (Malta) are linked with easterly flow. This connection

is well reflected by W-CCP3 and W-CCP4 for all coastal areas in this region exposed to the east or southeast. Thus, not only primary CCPs prove to be important, but also some of those with lower amounts of explained variance if looking at particular regions being less affected by major circulation patterns of a larger scale analysis. Furthermore, similar effects in different regions are assigned to different circulation patterns, e.g. increased precipitation for the extreme eastern Mediterranean to an easterly trough occurring in the positive mode of W-CCP3 compared with the MMC central trough favouring regions further upstream. Regional peculiarities are also included in W-CCP4 and W-CCP5, indicating that high pressure over eastern Europe without extension to the eastern Mediterranean itself is favourable for precipitation in this area due to the blocking action north of it.

Non-leading modes include further important aspects: e.g. W-CCP3 also shares some AO/NAO variance (Table III), but with a different pattern over Europe compared with W-CCP1. W-CCP4 closely resembles the most important CCA mode linked with precipitation variability across Europe (North Sea pattern of Qian *et al.* (2000)). W-CCP4 extends this North Sea pattern (valid for the SLP level) to an upper level (500 hPa), where an additional centre of variation appears around the Black Sea and Turkey. This pattern is reproduced within a Mediterranean context, but with reduced impact compared with its primary importance for European rainfall variability.

The strong downward trend in W-CCP4 (Table II) implies a shift towards higher pressure south of 45–50 °N and to lower pressure north of it during the winter months. This means a contribution of negative rainfall deviations for nearly the whole Mediterranean area since the 1970s and, at the same time (according to the first CCA mode of Qian *et al.* (2000)), above-normal winter precipitation for the rest of Europe becoming strongest in northern Europe.

W-CCP5 has the strongest correlation with the EA teleconnection pattern (Table III). Its influence on Mediterranean precipitation, however, is rather low, but note that, generally, a weakening of high-pressure systems in continental Europe (consistent with the negative mode of W-CCP5) is unfavourable for precipitation around the eastern Mediterranean basin.

A further synthesis is feasible with respect to temporal evolutions. Coupled patterns whose time series include distinct changes or trends (W-CCP4, W-CCP1, W-CCP2) imply pressure increases in southern (mainly subtropical) latitudes leading to widespread decreases in winter precipitation for most of the Mediterranean area. Thus, the general tendency towards more stable conditions in the Mediterranean winter months since the mid-1970s (Makrogiannis *et al.*, 1990; Schönwiese *et al.*, 1994; Reddaway and Bigg, 1996; Schönwiese and Rapp, 1997; Maheras *et al.*, 2000) is put into the perspective of large-scale circulation dynamics. These additionally imply decreasing pressure north of 55 °N (Schönwiese *et al.*, 1994; Schönwiese and Rapp, 1997) and a weakened influence of the Siberian anticyclone on continental Europe (Sahsamanoglou *et al.*, 1991). In particular, the developments of both W-CCP1 and W-CCP4 seem to be directly related to the climatic trends for Europe published by Schönwiese *et al.* (1994) and Schönwiese and Rapp (1997). The time series of W-CCP1 clearly reflects the recent evolution of the AO (Thompson *et al.*, 2000), the NAO (Hurrell and van Loon, 1997; Jacobeit *et al.*, 2001) and the MO (Conte *et al.*, 1989; Piervitali *et al.*, 1997), providing the dynamical background for the observed precipitation changes from the Atlantic regions up to the central parts of the Mediterranean area. At the same time, the opposite trend of increased precipitation in southern Israel (Ben-Gai *et al.*, 1994, 1998) becomes consistent in view of the upper cyclonic circulation downstream realized within the positive mode of W-CCP1.

5.2. Spring type

The first CCP during the spring months of April and May does not reproduce an MO pattern, but rather a modified MMC pattern with horizontal axes of its pressure centres of variation shifted to a southwest–northeast orientation (see W-CCP2 and SP-CCP1 in Figures 1 and 3, respectively). The MMC configuration, being related to Mediterranean cyclogenesis, is consistent with the spring maximum of cyclones moving in northeastward directions across one of the Mediterranean basins (Alpert *et al.*, 1990; Trigo *et al.*, 1999). Compared with W-CCP2, the precipitation pattern in spring is shifted somewhat to the northwest, thus affecting the eastern Mediterranean region less, which receives very little precipitation during these months. SP-CCP1 does not show any strong correlations to Northern Hemisphere teleconnection indices (Table III).

SP-CCP2 may be seen as a transitional MO pattern in between the winter (W-CCP1) and summer (S-CCP2) types of this pattern, thus indicating that the MO remains importance during the whole year but with varying ranks among the seasonal CCPs. The typical MO features known from wintertime are weakened and shifted in a northwesterly direction. The station pressure indices of the MO usually correlate best with this pattern during spring (Table IV), except for Conte's upper-level index, whose first station (Algiers) most distinctly differs from the primary pressure centre of SP-CCP2. The correlation coefficients of this pattern with particular AO and NAO time series (derived from EOF analyses) are lower than the corresponding ones during winter and summer (Table III). This is probably due to a major shifting of the NAO centres of action to the western Atlantic in spring (Wallace and Gutzler, 1981; Barnston and Livezey, 1987).

The circulation pattern of SP-CCP3 does not occur in winter, but shows some relations to W-CCP3 and W-CCP4, with the southern centres of variation having direct influence on the greatest part of the Mediterranean region (except the areas around the Adriatic Sea). The southwesterly regions, with decreasing spring precipitation during the last three decades (Jacobeit, 2000), mostly correspond to those areas in the southwestern part being affected by decreasing rainfall contributions due to the recent preference for positive SP-CCP3 modes.

During spring, the absence of patterns with high pressure over eastern Europe being positively correlated with precipitation in the eastern Mediterranean clearly indicates that this winter-type blocking pattern is no longer important during the transition from winter to summer.

5.3. Summer type

Circulation–rainfall relationships during summer are characterized by one particular pattern and by two further patterns representing seasonally adjusted modulations of patterns known from other seasons. Thus, S-CCP1 primarily constitutes the summer type of coupled variability, which is not reproduced during the remaining seasons. It has the biggest influence on summer precipitation for most of those regions in the Mediterranean domain which receive nonnegligible rainfall amounts during this season. Table III reveals that this pattern is strongly related to the Northern Hemisphere east Atlantic jet (EA-Jet) pattern appearing during the summer half year in the form of a zonally symmetric pressure seesaw between the northeastern Atlantic/Scandinavia and the Mediterranean Sea/North Africa. The positive S-CCP1 mode (linked to the negative EA-Jet mode) seems to be related to Mediterranean cyclone tracks in summer, which are mostly arranged from the western basin towards the Black Sea (Alpert *et al*., 1990; Trigo *et al*., 1999). The accumulation of positive modes between 1964 and 1978 led to increased precipitation amounts in relation to the S-CCP1 pattern, especially affecting the northern regions, the rainiest regions during the Mediterranean summer. Opposite conditions prevailed between 1980 and 1994 (strongest summer rainfall reductions in the wettest regions to the north due to enhanced anticyclonic conditions with negative S-CCP1 modes). A recent prominent case with a clear-cut positive mode of S-CCP1 occurred in August 2002, which was characterized by an anticyclonic anomaly above southern Scandinavia and distinctly unstable conditions in the northern Mediterranean area, even including Vb cyclone tracks, leading to exceptional flooding in parts of central Europe. Concomitantly, the time coefficient of the EA-Jet pattern dropped to one of its lowest values during this particular month (NOAA–CPC, 2003).

S-CCP2 represents a seasonal modulation of W-CCP1 and SP-CCP2 and, therefore, may be seen as a summer type of the MO pattern. This is supported by the zonally symmetric circulation pattern, as well as by significant correlations with AO and NAO (Table III). Compared with the other seasons, however, the western European centre is shifted slightly northward and its direct influence on Mediterranean precipitation is restricted to the far northwestern borders of this region. Owing to this seasonal modulation, the explained rainfall variance is reduced and correlations with fixed station indices of the MO fall off considerably (Table IV).

S-CCP3, being a weakened and slightly northward-shifted modification of SP-CCP3, has a reduced percentage of explained rainfall variance compared with the spring season; direct influences of the pressure centres of variation on Mediterranean rainfall are also weakened and reduced in their spatial extent.

Finally, the distinct effects of topography are no longer depicted during summer, indicating that subgrid-scale convection now dominates the rain-producing mechanisms.

6. CONCLUSIONS

The analyses have revealed different circulation regimes governing rainfall variability throughout the Mediterranean region during different seasonal periods. These regimes are not necessarily the same as those resulting from analyses that deal exclusively with circulation dynamics (e.g. Wallace and Gutzler, 1981; Barnston and Livezey, 1987), since it is the direct coupling with substantial parts of rainfall variability in different regions of the Mediterranean area that has been focused on within the present study. Thus, for example, variance of the EA pattern, identified by Wallace and Gutzler (1981) as a major Northern Hemispheric teleconnection system, is included in several different patterns, primarily W-CCP5 and W-CCP2. The seasonally different circulation regimes coupled with Mediterranean precipitation may be distinguished by means of the corresponding first modes, depicting for winter the MO pattern, for spring a modified version of the MMC pattern, and for summer an EA-Jet-related pattern. From another point of view, the canonical patterns may be distinguished between particular patterns for only one or two seasons and seasonally adjusted modulations of patterns recurring during all seasons. The former patterns include the EA-Jet-related pattern S-CCP1 for summer and the MMC pattern for winter and spring, these being of crucial importance for the whole central to eastern Mediterranean domain. The most important pattern, recurring with dynamical adjustments throughout the whole year, reflects the seasonal cycle of the MO, which can be described by varying properties of coupled patterns of pressure and precipitation variability: from winter (W-CCP1) to spring (SP-CCP2) and to summer (S-CCP2) the MO patterns show a gradual weakening in terms of the canonical correlation coefficients, the percentages of explained rainfall variances, the strengths of pressure deviation and the direct influence of pressure centres of variation on regional rainfall in the Mediterranean area. The MO patterns must not be seen, however, as independent large-scale circulation modes, since they correlate significantly with the Northern Hemisphere modes of the AO and NAO. On the other hand, they do not coincide with the AO/NAO, but rather comprise those parts of the AO/NAO being linked with Mediterranean precipitation variability. Both the MO and its connection to the AO/NAO are best developed during winter, fade away towards summer and recover afterwards. This seasonal cycle is well represented by the above-mentioned sequence of seasonally adjusted coupled patterns of variability. In terms of circulation dynamics, the MO turned out to be primarily an upper-level phenomenon, controlled by seasonally varying position and length of upper tropospheric long waves. Station indices of the MO (Table IV) are, therefore, less appropriate to catch dynamic MO variability outside the winter months and with respect to sea-level conditions.

Two major conclusions refer to the precipitation analysed. First, the gridded data with a 0.5° resolution (New *et al*., 2000) proved to be appropriate even for depicting the influence of topography on flow-dependent rainfall distribution patterns, i.e. areas near mountain ranges exposed to the prevailing flow resulting from a particular pressure pattern stand out against the other areas in terms of rainfall deviations. Second, recent rainfall trends, known from independent studies (e.g. Schönwiese and Rapp, 1997; Jacobeit, 2000), may be explained by temporal changes of some coupled patterns of variability, first of all concerning the winter season. Thus, the observed trend towards drier conditions in large parts of the Mediterranean area is linked to a change in W-CCP4 with preferred negative modes since the 1970s (increased pressure south of 45–50 °N), to a shift in the MMC pattern towards negative modes since the late 1980s (weakening of the central trough), and to the rising trend in the MO pattern (higher pressure in western and central parts of the Mediterranean area) being connected to the hemispheric circulation modes of the AO and NAO. The inverse conditions in the southeastern region are also compatible with the latter trend, since the positive mode of the MO pattern includes upper cyclonic components there. During spring, decreasing rainfall in the southwesterly regions corresponds to the recent preference for positive SP-CCP3 modes (increased pressure around this area). Annual to decadal anomalies of summer precipitation are linked to temporal variations of the EA-Jet-related pattern.

Altogether, the inclusion of the whole Mediterranean domain into the canonical analyses implies that different regional rainfall changes are integrated into an overall interrelation between rainfall patterns and large-scale atmospheric circulation dynamics.

REFERENCES

Adjez A. 2000. Changes in the rainfall regime in the North-African region: links with large-scale oscillation phenomena. In *Conference Abstracts 'Detection and modelling of recent climate change and its effects on a regional scale'*, Tarragona; 24.

Alpert P, Neeman BU, Shay-El Y. 1990. Intermonthly variability of cyclone tracks in the Mediterranean. *Journal of Climate* **3**: 1474–1487.

Amanatidis GT, Paliatsos AG, Repapis CC, Barttzis JG. 1993. Decreasing precipitation trend in the Marathon area, Greece. *International Journal of Climatology* **13**: 191–201.

Barnett T, Preisendorfer R. 1987. Origins and levels of monthly and seasonal forecasts skill for the United States surface air temperatures determined by canonical correlation analysis. *Monthly Weather Review* **115**: 1825–1850.

Barnston AG, Livezey RE. 1987. Classification, seasonality and persistence of low-frequency atmospheric circulation patterns. *Monthly Weather Review* **115**: 1083–1126.

Ben-Gai T, Bitan A, Manes A, Alpert P. 1994. Long-term changes in annual rainfall patterns in southern Israel. *Theoretical and Applied Climatology* **49**: 59–67.

Ben-Gai T, Bitan A, Manes A, Alpert P, Rubin S. 1998. Spatial and temporal changes in rainfall frequency distribution patterns in Israel. *Theoretical and Applied Climatology* **61**: 177–190.

Brunetti M, Maugeri M, Nanni T. 2000. Variations of temperature and precipitation in Italy from 1866 to 1995. *Theoretical and Applied Climatology* **65**: 165–174.

Brunetti M, Maugeri M, Nanni T. 2002. Atmospheric circulation and precipitation in Italy for the last 50 years. *International Journal of Climatology* **22**: 1455–1471.

Buffoni L, Maugeri M, Nanni T. 1999. Precipitation in Italy from 1833 to 1996. *Theoretical and Applied Climatology* **63**: 33–40.

Chbouki N, Stockton CW, Myers DE. 1995. Spatio-temporal patterns of drought in Morocco. *International Journal of Climatology* **15**: 187–205.

Conte M, Giuffrida S, Tedesco S. 1989. The Mediterranean oscillation: impact on precipitation and hydrology in Italy. In *Proceedings of the Conference on Climate and Water*, vol. 1. Publications of Academy of Finland: Helsinki; 121–137.

Corte-Real J, Zhang X, Wang X. 1995. Large-scale circulation regimes and surface climatic anomalies over the Mediterranean. *International Journal of Climatology* **15**: 1135–1150.

Corte-Real J, Qian B, Xu H. 1998. Regional climate change in Portugal: precipitation variability associated with large-scale atmospheric circulation. *International Journal of Climatology* **18**: 619–635.

Douguedroit A. 1998. Que peut-on dire d'une oscillation Méditerraneénne? In *Climate and Environmental Change*, Alcoforado MJ (ed.). Evora: 135–136.

Dünkeloh A, Jacobeit J. 2001. Zirkulationsdynamische Analyse mediterraner Niederschlagsanomalien und deren Entwicklungen in den letzten 50 Jahren. In *Proceedings of the Conference '20. Jahrestagung des AK Klima der Deutschen Gesellschaft für Geographie (DGfG)'*, Delemont; 51.

Esteban-Parra MJ, Rodrigo FS, Castro-Diez Y. 1998. Spatial and temporal patterns of precipitation in Spain for the period 1880–1992. *International Journal of Climatology* **18**: 1557–1574.

Flocas AA, Giles BD. 1991. Distribution and intensity of frontal rainfall over Greece. *International Journal of Climatology* **11**: 429–442.

González-Hidalgo JC, De Luis M, Raventós J, Sánchez JR. 2001. Spatial distribution of seasonal rainfall trends in a western Mediterranean area. *International Journal of Climatology* **21**: 843–860.

Goodess CM, Jones PD. 2002. Links between circulation and changes in the characteristics of Iberian rainfall. *International Journal of Climatology* **22**: 1593–1615.

Hotelling H. 1936. Relations between two sets of variates. *Biometrika* **28**: 321–377.

Hurrell JW. 1995. Decadal trends in the North Atlantic oscillation: regional temperature and precipitation. *Science* **269**: 676–679.

Hurrell JW. 2003. NAO index data (based on station data of Ponta Delgada, Azores, and Stykklsholmur/Reykjavik, Iceland; 1865–2003; monthly) provided by the Climate Analysis Section, NCAR, Boulder, USA. http://www.cgd.ucar.edu/~jhurrell/nao.stat.html [15 August 2003].

Hurrell JW, van Loon H. 1997. Decadal variations in climate associated with the North Atlantic oscillation. *Climatic Change* **36**: 301–326.

Jacobeit J. 1985. *Die Analyse großräumiger Strömungsverhältnisse als Grundlage von Niederschlagsdifferenzierungen im Mittelmeerraum*. Würzburger Geographische Arbeiten 63.

Jacobeit J. 1987. Variations of trough positions and precipitation patterns in the Mediterranean area. *Journal of Climatology* **7**: 453–476.

Jacobeit J. 2000. Rezente Klimaentwicklung im Mittelmeerraum. *Petermanns Geographische Mitteilungen* **144**(6): 22–33.

Jacobeit J, Dünkeloh A. 2003. Zirkulationsdynamik mediterraner Niederschlagsschwankungen — kanonische Korrelationsanalyse für das Winterhalbjahr seit Mitte des 20. Jahrhunderts. In *Beiträge zur Klima- und Meeresforschung*, Chmielewski FM, Foken Th (eds). Berlin and Bayreuth; 39–49.

Jacobeit J, Jonsson P, Bärring L, Beck C, Ekström M. 2001. Zonal indices for Europe 1780–1995 and running correlations with temperature. *Climatic Change* **48**: 219–241.

Jones PD. 2003. NAO Index Data (based on station data of Gibraltar and SW Iceland; 1821–2000; monthly) provided by Climatic Research Unit (CRU), Norwich, GB. http://www.cru.uea.ac.uk/cru/data/nao.htm [15 August 2003].

Jones PD, Jónsson T, Wheeler D. 1997. Extension to the North Atlantic oscillation using early instrumental pressure observations from Gibraltar and south-west Iceland. *International Journal of Climatology* **17**: 1433–1450.

Kalnay E, Kanamitsu M, Kistler R, Collins W, Deaven D, Gandin L, Iredell M, Saha S, White G, Woollen J, Zhu Y, Chelliah M, Ebisuzaki W, Higgins W, Janowiak J, Mo KC, Ropelewski C, Wang J, Leetmaa A, Reynolds R, Jenne R, Joseph D. 1996. The NCEP/NCAR 40-year reanalysis project. *Bulletin of the American Meteorological Society* **77**: 437–472.

Kistler R, Kalnay E, Collins W, Saha S, White G, Woollen J, Chelliah M, Ebisuzaki W, Kanamitsu M, Kousky V, van den Dool H, Jenne R, Fiorino M. 2001. The NCEP–NCAR 50-year reanalysis: monthly means CD-ROM and documentation. *Bulletin of the American Meteorological Society* **82**: 247–268.

Krichak SO, Tsidulko M, Alpert P. 2000. Monthly synoptic patterns associated with wet/dry conditions in the eastern Mediterranean. *Theoretical and Applied Climatology* **65**: 215–229.

Kutiel H, Kay PA. 1992. Recent variations in 700 hPa geopotential heights in summer over Europe and the Middle East, and their influence on meteorological factors. *Theoretical and Applied Climatology* **46**: 99–108.
Kutiel H, Paz S. 1998. Sea level pressure departures in the Mediterranean and the relationship with monthly rainfall conditions in Israel. *Theoretical and Applied Climatology* **60**: 93–109.
Kutiel H, Maheras P, Guika S. 1996a. Circulation and extreme rainfall conditions in the eastern Mediterranean during the last century. *International Journal of Climatology* **16**: 73–92.
Kutiel H, Maheras P, Guika S. 1996b. Circulation indices over the Mediterranean and Europe and their relationship with rainfall conditions across the Mediterranean. *Theoretical and Applied Climatology* **54**: 125–138.
Lamb PJ, Peppler RA. 1987. North Atlantic oscillation: concept and an application. *Bulletin of the American Meteorological Society* **68**: 1218–1225.
Littmann T. 2000. An empirical classification of weather types in the Mediterranean basin and their interrelation with rainfall. *Theoretical and Applied Climatology* **66**: 161–171.
Maheras P, Xoplaki E, Kutiel H. 1999. Wet and dry monthly anomalies across the Mediterranean basin and their relationship with correlation, 1860–1990. *Theoretical and Applied Climatology* **64**: 189–199.
Maheras P, Patrikas I, Karacostas Th, Anagnostopoulou Chr. 2000. Automatic classification of circulation types in Greece: methodology, description, frequency, variability and trend analysis. *Theoretical and Applied Climatology* **67**: 205–223.
Maheras P, Flocas HA, Patrikas I, Anagnostopoulou Chr. 2001. A 40 year objective climatology of surface cyclones in the Mediterranean region: spatial and temporal distribution. *International Journal of Climatology* **21**: 109–130.
Makrogiannis TJ, Sahsamanoglou CS. 1990. Time variation of the mean sea level pressure over the major Mediterranean area. *Theoretical and Applied Climatology* **41**: 149–156.
Meteorological Office. 1962. *Weather in the Mediterranean, General Meteorology*, vol. 1. Publication 391. HMSO: London.
Meyrhöfer S, Rapp J, Schönwiese CD. 1996. Observed three-dimensional climate trends in Europe 1961–1990. *Meteorologische Zeitschrift* **5**: 90–94.
New MG, Hulme M, Jones PD. 1999. Representing twentieth century space–time climate variability. Part I: development of a 1961–1990 mean monthly terrestrial climatology. *Journal of Climate* **12**: 829–856.
New MG, Hulme M, Jones PD. 2000. Representing twentieth century space–time climate variability. Part II: development of a 1901–1996 monthly terrestrial climate fields. *Journal of Climate* **13**: 2217–2238.
Nicholls N. 1987. The use of canonical correlation to study teleconnections. *Monthly Weather Review* **115**: 393–399.
NOAA–CPC. 2003. Northern Hemisphere teleconnection indices (1950–2003; monthly). http://www.cpc.ncep.noaa.gov/data/teledoc/telecontents.html [15 August 2003].
Palutikof J. 2003. Analysis of Mediterranean climate data: measured and modelled. In *Mediterranean Climate — Variability and Trends*, Bolle HJ (ed.). Springer Verlag: Berlin; 133–153.
Palutikof J, Conte M, Mendes JC, Goodess CM, Esprito Santo F. 1996. Climate and climatic change. In *Mediterranean Desertification and Land Use*, Brandt CJ, Thornes JB (eds). Wiley: Chichester; 43–86.
Piervitali E, Colacino M, Conte M. 1997. Signals of climatic change in the central–western mediterranean basin. *Theoretical and Applied Climatology* **58**: 211–219.
Qian B, Corte-Real J, Xu H. 2000. Is the North Atlantic oscillation the most important atmospheric pattern for precipitation in Europe? *Journal of Geophysical Research* **105**: 11 901–11 910.
Quadrelli R, Pavan V, Molteni F. 2001. Wintertime variability of the Mediterranean precipitation and its links with large-scale circulation anomalies. *Climate Dynamics* **17**: 457–466.
Reddaway JM, Bigg GR. 1996. Climatic change over the Mediterranean and links to the more general atmospheric circulation. *International Journal of Climatology* **16**: 651–661.
Reiter ER. 1975. *Handbook for Forecasters in the Mediterranean. Part I: General Description of the Meteorological Processes*. Naval Environmental Research Facility: Monterey, CA.
Rodó X, Baert E, Comin FA. 1997. Variations in seasonal rainfall in southern Europe during the present century: relationships with the North Atlantic oscillation and the El Nino–southern oscillation. *Climate Dynamics* **13**: 275–284.
Sahsamanoglou H, Makrogiannis T, Kallimopoulos P. 1991. Some aspects of the basic characteristics of the Siberian anticyclone. *International Journal of Climatology* **11**: 827–839.
Schönwiese CD, Rapp J. 1997. *Climate Trend Atlas of Europe — Based on Observations 1891–1990*. Kluwer Academic Publishers: Dordrecht.
Schönwiese CD, Rapp J, Fuchs T, Denhard M. 1994. Observed climate trends in Europe 1891–1990. *Meteorologische Zeitschrift* **3**: 22–28.
Steinberger EH, Gazit-Yaari N. 1996. Recent changes in spatial distribution of annual precipitation in Israel. *Journal of Climate* **9**: 3328–3336.
Thompson DWJ, Wallace JM. 2000. Annular modes in the extratropical circulation. Part I: month-to-month variability. *Journal of Climate* **13**: 1000–1016.
Thompson DWJ, Wallace JM, Hegerl GC. 2000. Annular modes in the extratropical circulation. Part II: trends. *Journal of Climate* **13**: 1018–1036.
Thompson DWJ, Wallace JM. 2003. AO index data (based on the leading empirical orthogonal function (EOF); 1899–2002, monthly). http://www.atmos.colostate.edu/ao/Data/ao_index.html [15 August 2003].
Trigo RM, DaCamara CC. 2000. Circulation weather types and their influence on the precipitation regime in Portugal. *International Journal of Climatology* **20**: 1559–1581.
Trigo IF, Davies TD, Bigg GR. 1999. Objective climatology of cyclones in the Mediterranean region. *Journal of Climate* **12**: 1685–1696.
Trigo IF, Davies TD, Bigg GR. 2000. Decline in Mediterranean rainfall caused by weakening of Mediterranean cyclones. *Geophysical Research Letters* **27**: 2913–2916.
Türkes M. 1996. Spatial and temporal analysis of annual rainfall variations in Turkey. *International Journal of Climatology* **16**: 1057–1076.
Von Storch H, Zwiers FW. 1999. *Statistical Analysis in Climate Research*. Cambridge University Press: Cambridge.

Von Storch H, Zorita E, Cubasch U. 1993. Downscaling of global climate change estimates to regional scales: an application to Iberian rainfall in wintertime. *Journal of Climate* **6**: 1161–1171.

Wallace JM, Gutzler DS. 1981. Teleconnections in the geopotential height field during the Northern Hemisphere winter. *Monthly Weather Review* **109**: 784–812.

Xoplaki E, Luterbacher J, Burkard R, Patrikas I, Maheras P. 2000. Connection between the large-scale 500 hPa geopotential height fields and precipitation over Greece during wintertime. *Climate Research* **14**: 129–146.

Xoplaki E, González-Rouco JF, Luterbacher J, Wanner H. 2003. Mediterranean summer air temperature variability and its connection to the large-scale atmospheric circulation and SSTs. *Climate Dynamics* **20**: 723–739.

Zorita E, Kharin V, von Storch H. 1992. The atmospheric circulation and sea surface temperature in the North Atlantic area in winter: their interaction and relevance for Iberian precipitation. *Journal of Climate* **5**: 1097–1108.